*IOSR Journal of Electrical and Electronics Engineering (IOSR-JEEE)*
*e-ISSN: 2278-1676,p-ISSN: 2320-3331, Volume 11, Issue 6 Ver. III (Nov. – Dec. 2016), PP 11-18*
*www.iosrjournals.org*

# Fabrication and Characterization of Zn-doped CdTe nanoparticles based Dye sensitized solar cells

Swades Ranjan Bera* [a], Satyajit Saha [a]
[a]*Department of Physics and Technophysics, Vidyasagar University, Midnapore-721102, West Bengal, India*

***Abstract:*** *In the present work, undoped and Zn-doped CdTe nanoparticles are grown by chemical reduction method. The grown synthesized nanoparticles are characterized structurally by X-Ray diffraction (XRD) and transmission electron microscopy (TEM). The X-ray diffraction study confirmed the crystal structure of undoped and Zn-doped CdTe nanoparticles. Transmission electron microscopy study indicates the nature and size of the nanoparticles. The grown nanoparticles are characterized optically by Optical Absorption, Photoluminescence (PL) studies. The optical properties of the dye are also studied. The extraction of Hibiscus mutabilis is used as a natural dye. Also photoconductivity study shows the change of photosensitivity and relaxation time with doping. Dye sensitized solar cells based on doped as well as undoped CdTe have been fabricated and characterized through J-V study at dark and under illumination of light condition. The measurement of efficiency and fill factor, open circuit voltage and short circuit current density of the dye sensitized solar device are also carried out.*

***Keywords:*** *Structural properties, Optical properties, undoped and Zn-doped CdTe, Photorelaxation time, J-V characteristics, DSSCs.*

## I. Introduction

Semiconductor nanoparticles (NPs) have scientific community. It exhibits many interesting properties and it also has a tremendous potential for the industrial applications in many technical fields including photo catalysts, gas sensors, biological detection and imaging, solar cells, photo detectors and UV sensors, nonlinear optical materials, short-wavelength laser diodes, various luminescence devices, etc [1-5]. Due to their excessive surface-to-volume ratio, good optical characteristics, high electron-transfer efficiency, quantum confinement effect, biocompatibility, dimensional similarities with biological macromolecules and high surface reaction activity is likely to be observed in nanoparticles [6-11]. And due to the confinement defect various novel properties like structural, optical, electrical, magnetic etc. are coming out of various nanomaterials. As a direct wide gap semiconductor ($E$g = 1.58 eV at room temperature), CdTe is the primary semiconductor material for room temperature the high quality of the resulting sample, the fact that the optical gap lies in the visible range, has a high optical absorption coefficient [12]( $> 10^4$ $cm^{-1}$) and large Bohr radius [13] (10 nm in bulk [14]).The understanding of many properties of semiconductor nanoparticles can be achived by going beyond the pure nanoparticles and investigate materials that are intentionally doped with impurities [15-23]. One of the advantages of this material is the possibility to vary its band gap by introducing a dopant [24]. We have selected Zn as dopant because of its similar structure of the electronic cell to those of Cd. Also Cd in CdTe can be easily substituted by Zn under appropriate condition [25-27]. The purpose of the present paper is to study the effects of dopant on the structural, electrical, and optical properties of CdTe nanoparticles. The change in optical, structural, electrical properties of CdTe is produced by Zn-doping.

## II. Experimental Section

### 1. Materials:

Anhydrous Cadmium Chloride ($CdCl_2$), Tellurium Powder (Te), Sodium Borohydride ($NaBH_4$), Ethylenediamine (EN, $NH_2CH_2CH_2NH_2$), Zinc Chloride ($ZnCl_2$), Indium Tin Oxide (ITO) coated glass, glass plate, Ethanol, $I_2$, Potassium Iodide and Graphite paint was purchased from Merck, India. All materials were used as starting materials without any purification.

### 2. Materials Preparation:

Anhydrous $CdCl_2$, Tellurium powder, sodium borohydride and Ethylenediamine (EDA) have been taken to prepare samples at ratio 1:1:2. An amount 382.8 mg of Te powder was added to a conical flask containing 45 mL of ethylenediamine (EDA). After being stirred magnetically for 10 min, 603.96 mg of $CdCl_2$ was added to the flask. After 5 minutes, 227 mg of $NaBH_4$ was added into this solution and the magnetic stirring is continued for 4 hours. 4mg of $ZnCl_2$ was added to this solution after 2 hours the ingredients were mixed and stirring is continued. After the mixture was stirred for 4h, a blackish precipitate formed, which was filtered and then washed with distilled water in sequence several times to remove possible impurities such as

excess Tellurium. Then the washed precipitates were collected in a clean petridish and finally dried in vacuum at room temperature for 24 hour and collected for characterization. Same procedure is followed without adding ZnCl2 leads to the formation of undoped CdTe.

**3. CdTe Film fabrication for photoconductive measurement:**

For photoconductive measurement, thin films of the undoped CdTe and Zn-doped CdTe have been grown from the dispersed sample. The glass substrate has been dipped in the dispersed solution at least for 3 days. Thin film of CdTe is uniformly deposited on the glass substrate. Graphite paint is used as ohomic contact for measurement of I-V characteristics.

**4. Device Fabrication for dye synthesis solar cell:**

Hibiscus mutabilis flower (Land lotus flower) is collected from garden of Vidyasagar University campus, West Bengal, India. The fresh flowers are washed in distilled water for several times and placed in a vacuum furnace for 2 hours. After drying, the flowers are crushed to extract with a porcelain mortar and pestle. Crushed sample is dissolved with 40mL of ethanol without exposure of light. After extraction, they are filtered by filtered paper. This is the solution of Anthocyanin which is extracted from the Hibiscus mutabilis. Next, 0.4 gm of undoped and 0.4 gm Zn-doped CdTe nanoparticles are separately added with 0.5 mL acetic acid and grinding in mortar for lump free pestle. The CdTe paste is prepared. A uniform layer of undoped and Zn-doped CdTe paste is deposited on the conducing surface of ITO glass. Undoped and Zn-doped CdTe layer on conductive glass is heated in a furnace at 40° C for one hour. This glass plate has placed in anthocyanin solution for 10 minutes. The conducing surface of other ITO glass plate is coated with graphite paint as a counter electrode. The two electrodes are then sandwiched together using two binder clips. A redox electrolyte is prepared using 0.5 mol of KI, 0.05mol of $I_2$, and 0.5 mol of acetic acid. 2-3 drops of redox electrolyte solution have been injected into the interspaced between the cells to serve as a conductor to electrically connect the two electrodes.

**5. Materials Characterization:**

The X-ray diffraction (XRD) pattern on the samples were recorded by a X-ray diffractometer (miniflex II, desktop-X-ray diffractometer) using Cu-kα radiation of wavelength $\lambda = 1.54\ A^0$ for 2θ ranging from $20^0$ to $70^0$. The Transmission Electron Micro-graph of the as-prepared samples has been taken using a JEOL-JEM-2010 transmission electron microscope operating at 200 kV. Selected area electron diffraction (SAED) pattern of the said nanoparticles were also performed. Optical absorption measurements of the dispersed samples have been studied in the range of 300 nm–700 nm using a Shimadzu Pharmaspec 1700 UV–VIS Spectrophotometer. PL spectra of the dispersed samples are recorded using Perkin Elmer LS 55 Fluorescence Spectrophotometer. The photoelectrical characteristics have been studied using Keithley electrometer- 6514. From long time photoconductive decay, relaxation time has been measured. Intensity of light falling on the sample is measured by luxmeter and found to be 50 lux. Photovoltaic cells of dye synthesis (DSSCs) using natural dyes as sensitizers were performed by measuring the current density-voltage (J-V) curves in ethanol solvent under illumination with white light (100 mW $cm^{-2}$).

## III. Results And Discussions

**1. Structural Properties using XRD:**

Fig. 1 shows the XRD pattern of the synthesized grown undoped CdTe and Zn-doped CdTe. All the diffraction peaks come mainly from the cubic phase of CdTe. The XRD diffraction peaks are indexed as CdTe in cubic phase (111), (200), (220), (311), (222), (400), (331) and (420) as per JCPDS card 75-2083 whereas some peaks (110), (112) and (022 related to hexagonal phase in agreement with JCPDS card 80-0089 are also found. No additional peak is observed after doping which indicates absence of any possible secondary phase related to the impurity atom. Average particle size of crystallites is calculated by Debye Scherer equation

$$P = k\lambda/\beta\cos\theta$$

Where k is the shape factor, the dimensionless, shape factor has typical value 0.9, λ is the X-ray wavelength 0.154 nm, β is the line broadening at half maximum intensity (FWHM) in radians, θ is the Bragg angle and P is the mean size of the ordered domains. Average sizes of undoped and Zn-doped CdTe calculated from Debye Scherer equation are 34.9 nm for undoped CdTe and 37.1 nm for Zn-doped CdTe. So, the size of CdTe nanoparticles increased after Zn doping.

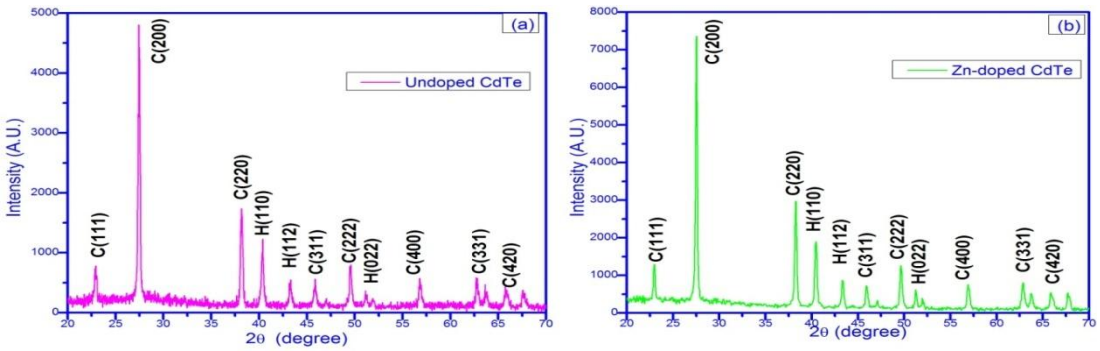


**Fig. 1** XRD pattern of as prepared undoped and Zn-doped CdTe nanostructure

**2. Morphological study using TEM:**

Morphologies of the synthesized undoped and Zn-doped CdTe at fixed reactional temperature are shown in fig 2. The diameter of the nanoparticles is 27.5 nm and 37 nm for undoped and Zn-doped CdTe respectively. The particle sizes increases due to Zn dopant. This is probably due to the stretching of the surface with the inclusion. Selected area electron diffraction (SAED) pattern indicates that crystallinity is good for Zn doped CdTe. The nanoparticles sizes are shown in table-1.

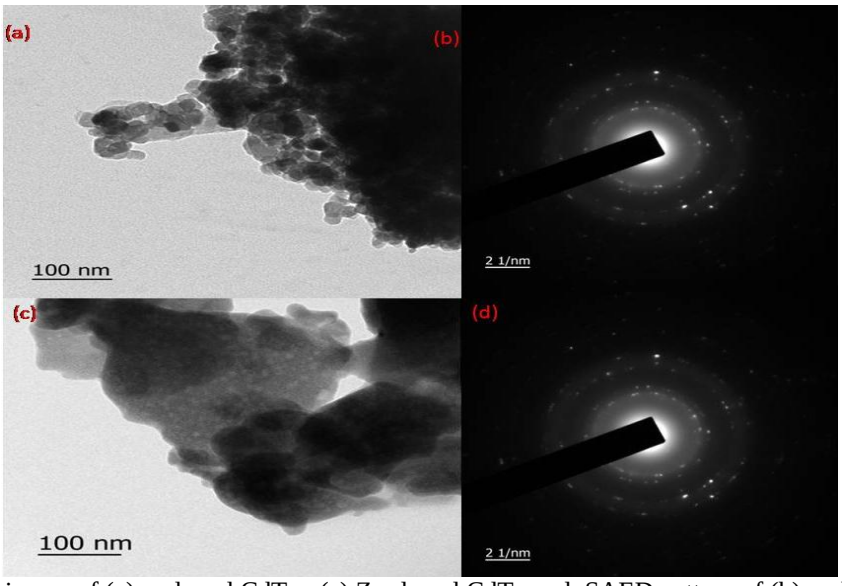


**Fig. 2** HRTEM image of (a) undoped CdTe , (c) Zn-doped CdTe and SAED pattern of (b) undoped CdTe , (d) Zn-doped CdTe

**Table:-1:** Determination of size, shape and band gap of undoped and Zn-doped CdTe nsnostructure

| **Name of Samples** | **Shape of Nanostructure** | **Average Size of the Nanostructure (From TEM) (nm)** | **Band Gap (eV)** | Relaxation Time (Sec) | Photosensitivity |
|---|---|---|---|---|---|
| Undoped CdTe | Spherical nanoparticles | Diameter-27.5 | 2.19 | 54.05 | 1.2171 |
| Zn-doped CdTe | Spherical nanoparticles | Diameter- 37 | 2.08 | 65.82 | 1.2636 |

**2. Optical Properties of CdTe nanostructure:**

Optical properties of CdTe samples were determined through UV-VIS absorbance spectroscopy and photoluminescence studies. The CdTe nanomaterials were dispersed in Toluene using ultrasonication for 20 minutes for UV-VIS absorption measurements. Fig – 3 shows the optical absorbance spectra of undoped and Zn-doped CdTe samples. The band gap of the as- prepared nanoparticles is determined by using the Tauc's relation [28] $(\alpha h\nu) = C\ (h\nu - \Delta E_g)^{1/2}$ where C is a constant, α is the absorption coefficient, hν is the photon energy, $E_g$ is the band gap of the material. Fig -4 shows the plot of $(\alpha h\nu)^2$ vs. energy (hν) and it is used to determine band gap. The linear part of the curve is extrapolated to energy (hν) axis to determine band gap. The band gap is found to be 2.19 eV for undoped CdTe and 2.08 eV for Zn-doped CdTe. At each growth condition

band gap is found to be greater than the bulk value and this indicates quantum confinement. Band gap of Zn-doped CdTe is smaller than that of undoped CdTe.

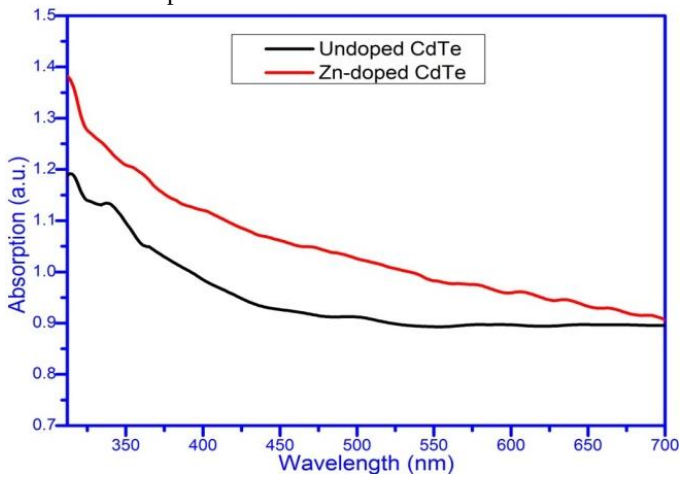


**Fig. 3** Plot of optical absorption spectra of as prepared undoped and Zn-doped CdTe nanostructure

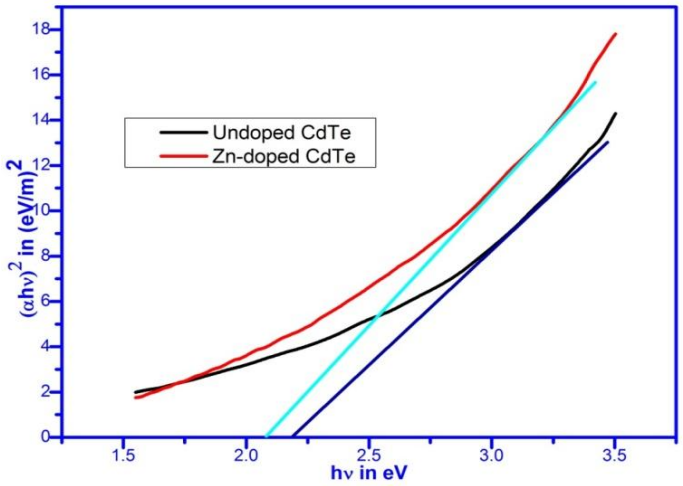


**Fig. 4** Plot of $(\alpha h\nu)^2$ vs. $(h\nu)$ to determine band gap of undoped and Zn-doped CdTe

**4. Optical Properties of Hibiscus mutabilis extract dye:**

Optical properties of natural dye molecules utilized in scientific and technological applications can strongly depends on properties of the surrounding media and the interaction of the dancing molecules. Absorbance spectra provide necessary information on the absorption between the dye ground state and excited states. Hence it provides information about solar energy range. The extraction of Hibiscus mutabilis is the natural dye molecules. The optical absorbance spectra of the prepared Hibiscus mutabilis extract in ethanol is shown in fig.5. Ethanol is the appropriate solvent in the extraction of phenolic compounds from plant tissues. Such solvent effects mainly the interaction of dye molecules to the solvent surroundings which depends on the enhanced forces which can be determined by the charge distribution of the ethanol and dye molecules [29-30].

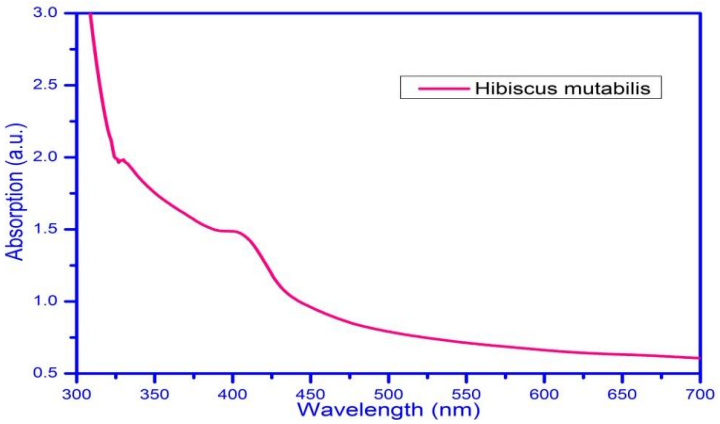


**Fig. 5** Plot of optical absorption spectra of Hibiscus mutabilis extract

**5. Photoluminescence Properties of CdTe nanostructure**

The photoluminescence (PL) experiment is employed to study the optical response of samples and the spectrum taken at room temperature is shown in Fig 6. The PL spectra were measured with excitation wavelength 360 nm of the undoped and Zn-doped CdTe. PL peak shifts slightly towards higher wavelength with Zn doped which is in agreement with the absorption result. Also peak position indicates that luminescence occur in each case from the state close to the band gap.

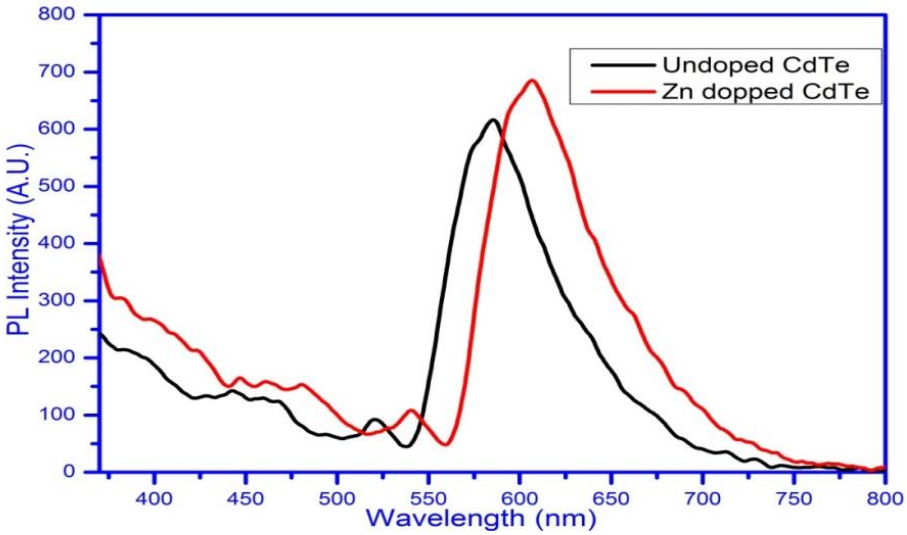


**Fig. 6** Plot of photoluminescence intensity of as prepared undoped and Zn-doped CdTe nanostructure

**6. Photoconductivity of undoped and Zn-doped CdTe Nanoparticles:-**

The growth and decay of photocurrent of undoped and Zn-doped CdTe is shown in Fig. 7. When the steady current is reached then the light source is off. Relaxation times of undoped and Zn-doped CdTe are measured from long time photo decay curve. Relaxation time is measured using the relation

$\Delta n = \Delta n_s \exp(-t/\tau)$

Where $\Delta n$ is the excess carrier concentration at any arbitrary time, $\Delta n_s$ is the excess carrier concentration at steady state condition and $\tau$ is relaxation time.

This above relation can be correlated to experimentally measurable parameter by

$\Delta n_s/\Delta n = \Delta Iph(s)/\Delta Iph(t) = \exp(t/\tau)$

$\Delta Iph(s)$ is the change in photocurrent at steady state condition with respect to dark current value. $\Delta Iph(t)$ is the change in photocurrent at an arbitrary time $t$ with respect to the dark. The plot of ln $(\Delta Iph(s)/\Delta Iph(t))$ vs. $t$ gives the straight line as shown in fig 7(b) and 7(d). From the slope of the respective curve, the long time relaxation is estimated as shown in table 1. Experimental results show that the lower band gap energy Zn-doped CdTe having greater relaxation time and higher band gap energy undoped CdTe having lower relaxation time. This is probably due to the decrease of surface states with the increase of grain size [31].

Nanomaterials photosensitivity $(I_L - I_D)/I_D$ of undoped and Zn-doped CdTe thin films is another important parameter used for photosensitive devices performance [32]. In this regards the following relation is

used $\Delta Iph(s) = I_L - I_D$, where $I_L$ and $I_D$ are currents under illumination and in dark respectively. The variations of photosensitivity are a function of the impurity doping. It is observed from the figures 7(b) and 7 (d) that photosensitivity increases with Zn-doped CdTe thin films, which may be attributed to a decrease in the density of defect states after $ZnCl_2$ addition.

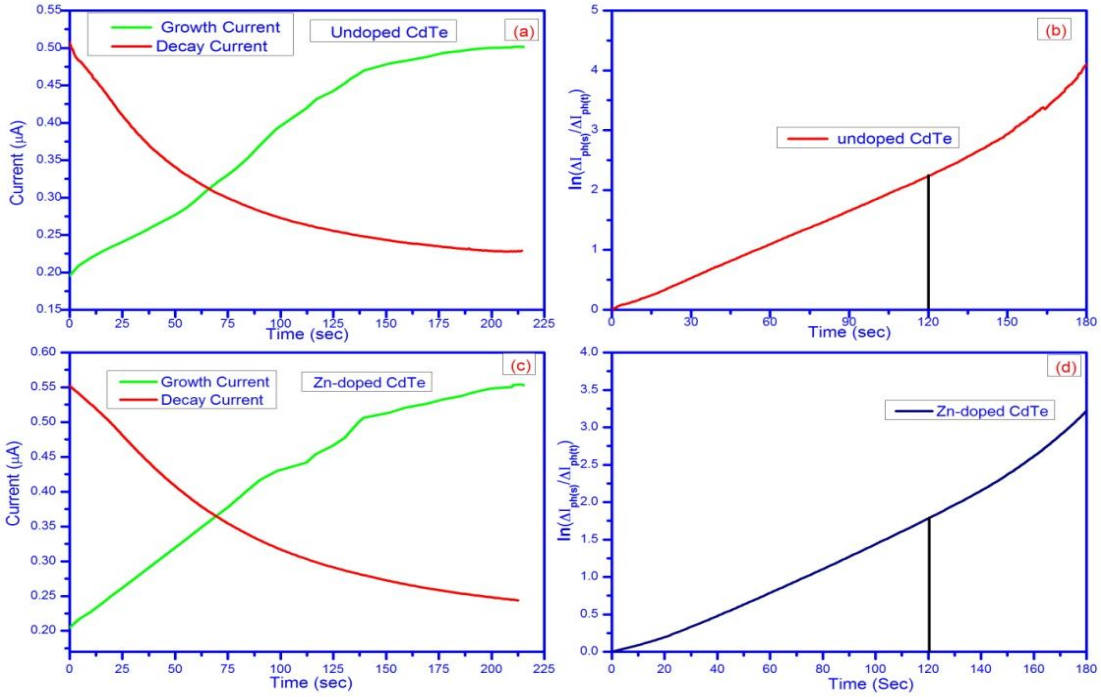


**Fig.7** The photoconductive growth, decay current and determination of relaxation time graph for undoped and Zn-doped CdTe samples

**7. Current density (J)–voltage (V) and power density (P)–voltage (V) characteristics:**

The extracted of Hibiscus mutabilis natural dye is sensitized to undoped and Zn-doped CdTe layer and dye synthesis solar cells have been fabricated. The fabricated solar cells have been characterized for J-V under dark and in illumination of visible light. Current density (J) – Voltage curves of DSSCs gives the important information on the photoelectric operational parameters as open circuit voltage, short circuit current, maximum power of the prepared DSSCs. Figure 8 (a) shows J-V characteristics of Hibiscus mutabilis natural dye sensitized solar cell undoped and Zn-doped CdTe in dark. It can be seen that the J-V curve shows the formation of solar cell in dark and under light illumination with increased current density with respect to dark, due to electron hole pair generated with absorption of light from dye confirming the light absorption by Hibiscus mutabilis natural dye. Fill Factor and efficiency of the photovoltaic devices are determined from J-V characteristics. Fill factor and efficiency can be calculated from the relation given below

$$FF = \frac{V_{max}\, J_{max}}{V_{oc}\, J_{sc}} \qquad \text{And} \qquad \eta = \frac{J_{sc}\, V_{oc}\, FF}{P_{in}}$$

Where, $V_{mp}$, $J_{mp}$ are Voltage and current density at maximum power. $V_{oc}$, $J_{sc}$ are open circuit voltage and short circuit current respectively, $P_{in}$ is the incident power and η is the efficiency. Fill factor is determined from the J-V characteristics. Open circuit voltages of undoped and Zn-doped CdTe in ethanol are 0.50V and 0.57V respectively. Short circuit current densities of undoped and Zn-doped CdTe in ethanol are 2.9667 mA and 3.264 mA respectively.

Power density (P) – Voltage (V) curve gives the important information on the photoelectric operational parameters. Figure 8(b) shows the power density (P) vs voltage (V) curve of undoped and Zn-doped CdTe. The maximum power efficiency (η%) of prepared DSSCs are 1.2038 and 1.5530 respectively. Zn-doped CdTe nanoparticles as photoanodes in DSSCs, and an enhancement in the conversion efficiency of DSSCs was achieved as compared to undoped CdTe nanoparticle-based DSSCs. DSSCs with undoped and Zn-doped CdTe nanoparticles films sensitized by Hibiscus mutabilis natural dye have been assembled and the comparison of photovoltaic properties is presented in Table 2. It can be seen that the Isc and the Voc for the DSSC constructed using the Zn-doped CdTe films show obvious improvement over the DSSC constructed using the undoped CdTe films. Doping CdTe with Zn influences to an increase of charge carrier density and the changing of Fermi energy levels. Therefore, the electron transport capacity of the CdTe is enhanced, and thus the higher Isc is

obtained. As a result, the conversion efficiency (η) is higher due to higher $I_{sc}$ [33]. So, due to improved Isc and $V_{oc}$, the Zn-doped CdTe nanoparticle-based DSSC attained a total power conversion efficiency of 1.5530%, which is larger compared to that of the undoped CdTe sample based DSSC (1.2038%).

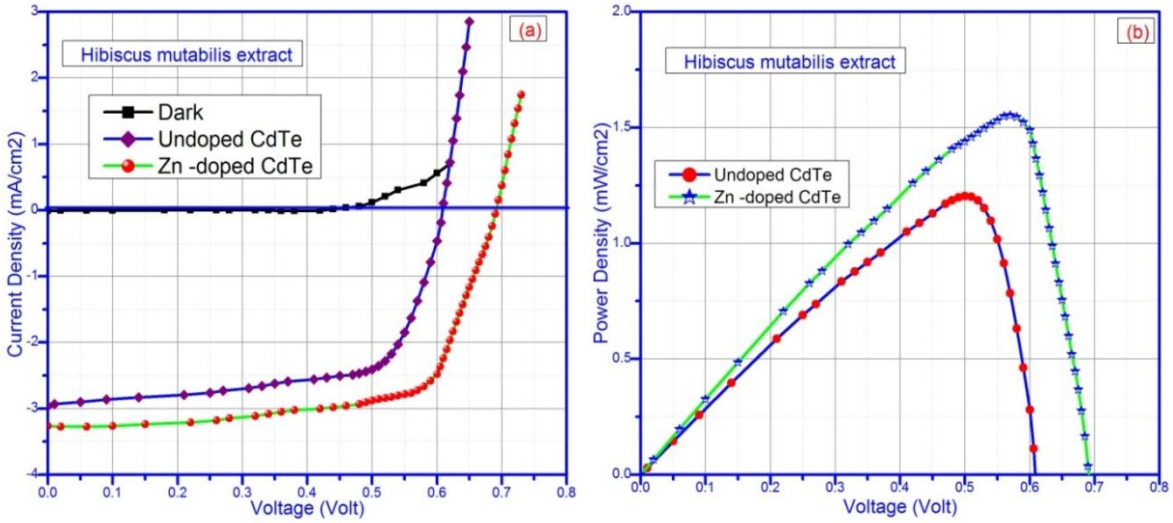


**Fig. 8**(a) Current density (J) vs applied bias (V) characteristics, (b) Power density (P) vs. voltage (V) plot of light of undoped and Zn-doped CdTe in dark and under illumination of light.

**Table:-2** Different Parameters Dye Sentisized Solar Cell Obtained From J-V Characteristics

| Anthocyanin | Samples | $V_{max}$(Volt) | $J_{max}$(mA/cm$^2$) | $V_{oc}$(Volt) | $J_{sc}$(mA/cm$^2$) | FF (%) | Efficiency(η)% |
|---|---|---|---|---|---|---|---|
| Hibiscus mutabilis | Undoped CdTe | 0.5 | 2.4076 | 0.609 | 2.9667 | 66.63 | 1.2038 |
| | Zn-doped CdTe | 0.57 | 2.7246 | 0.692 | 3.2640 | 68.76 | 1.5530 |

## IV. Conclusion

Undoped and doped CdTe nanoparticles are grown and characterized. Doping increases photosensitivity due to reduced recombination. Natural dye as Hibiscus mutabilis extract (Land lotus flower) is used in the fabrication of dye sensitized solar cell. Also efficiency of the DSSC can be improved by Zinc doping. The fabrication process of the device is simple and cost effective.

## Acknowledgements

Authors are acknowledging UGC and DST for supporting department of Physics and Technophysics of Vidyasagar University with various instrumental facilities through SAP and FIST programme.

## References

[1]. Singh VP, McClure JC (2003) Design issues in the fabrication of CdS–CdTe solar cells on molybdenum foil substrates. Sol Energy Mater Sol Cells 76:369–385
[2]. Duan X, Niu C, Sahi V, Chen J, Parce JW, Empedocles S, Goldman JL (2003) High-performance thin film transistors using semiconductor nanowires and nanoribbons. Nature 425:274–278. doi:10.1038/nature01996
[3]. Bera SR and Saha S. , Fabrication of CdTe/Si heterojunction solar cell, 2016, Applied Nanoscience , DOI 10.1007/s13204-015-0516-5
[4]. Capper P., Ed., Narrow Gap II-VI Compounds for Optoelectronic and Electromagnetic Applications, Chapman & Hall, London, UK, 1st edition, 1997.
[5]. Lovergine N., Prete P., Tapfer L., Marzo F., and Mancini M., "Hydrogen transport vapour growth and properties of thick CdTe epilayers for RT X-ray detector applications," Crystal Research and Technology, vol. 40, no. 10-11, pp. 1018–1022, 2005.
[6]. Rao C. N. R., Kulkarni G. U., Thomas P. J., Edwards P. P., Metal nanoparticles and their assemblies, Chem Soc Rev 29,27–35(2000); doi: 10.1039/A904518J
[7]. Bard A. J., Ding Z, Myung N., Electrochemistry and electrogenerated chemiluminescence of semiconductor nanocrystals in solutions and in films, Struct Bond 118,1–57(2005); doi: 10.1007/b137239
[8]. Bönnemann H., Richards R. M., Nanoscopic metal particles synthetic methods and potential applications, Eur J Inorg Chem 10:2455–2480(2001); doi: 10.1002/1099-0682(200109)
[9]. Alivisatos P., The use of nanocrystals in biological detection, Nat Biotechnol 22,47– 52(2004); doi:10.1038/nbt927
[10]. Riegler J., Nick P., Kielmann U., Nann T., Visualizing the self-assembly of tubulin with luminescent nanorods, J Nanosci Nanotech 5,380–385(2003); doi: org/10.1166/jnn
[11]. Medintz I. L., Uyeda H. T., Goldman E. R., Mattoussi H . , Quantum dots bioconjugates for imaging, labelling and sensing, Nat Mater 6,435–446(2005); doi:10.1038/nmat1390
[12]. Lane D., "A review of the optical band gap of thin film CdSxTe1−x," Solar Energy Materials and Solar Cells, vol. 90, no. 9, pp. 1169–1175, 2006.
[13]. Shokhovets, S., Ambacher, O., and Gobsch, G., Conduction-band dispersion relation and electron effective mass in III-V and II-VI zinc-blende semiconductors, Physics Review B: Condensed Matter Materials Physics, 76, 125203 (2007).

[14]. Mackowski, S., 'CdTe/ZnTe quantum dots-growth and optical properties' Thin Solid Films, 412, 96- 106 (2002).
[15]. Levy L., Hochepied J. F., Pileni M. P., Control of the Size and Composition of Three Dimensionally Diluted Magnetic Semiconductor Clusters, J Phys Chem 100,18322- 18326 (1996); doi: 10.1021/jp960824w
[16]. Mikulec F. V., Kuno M., Bennati M., Hall D. A., Griffin R. G., Bawendi M. G., Organometallic Synthesis and Spectroscopic Characterization of Manganese-Doped CdSe Nanocrystals, J Am Chem Soc 122, 2532–2540 (2000); doi: 10.1021/ja991249n
[17]. Malik M. A., Brien P. O., Revaprasadu N., Synthesis of TOPO-capped Mn-doped ZnS and CdS quantum dots, J Mater Chem 11,2382(2001); doi: 10.1039/b102709n
[18]. Norris D. J., Yao N., Charnock F. T., Kennedy T. A., High-Quality Manganese-Doped ZnSe Nanocrystals, Nano Lett 1,3-7,(2001); doi: 10.1021/nl005503h
[19]. Hanif K. M., Meulenberg R. W., Strouse G. F., Magnetic Ordering in Doped Cd1-xCoxSe Diluted Magnetic Quantum Dots, J Am Chem Soc 124,11495(2002); doi: 10.1021/ja0262840
[20]. Stowell C. A., Wiacek R. J., Saunders A. E., Korgel B. A., Synthesis and Characterization of Dilute Magnetic Semiconductor Manganese-Doped Indium Arsenide Nanocrystals, Nano Lett 3, 1441–1447 (2003); doi: 10.1021/nl034419+
[21]. Erwin S. C., Zu L. J., Haftel M. I., Efros A. L., Kennedy T. A., Norris D. J., Doping semiconductor nanocrystals, Nature 436,91-94(2005); doi:10.1038/nature03832
[22]. Kwak W. C., Sung Y. M., Kim T. G., Chae W. S. , Synthesis of Mn-doped zinc blende CdSe nanocrystals, Appl Phys Lett 90,173111(2007); doi.org/10.1063/1.2731682
[23]. Li L., Lu Y., Cai X. Y., Cheng Y., Ding Y.P., Synthesis of Mn-doped CdTe nanoparticles and their application as fluorescence sensors, The 14th International Meeting on Chemical Sensors, IMCS 2012, DOI 10.5162/IMCS2012/P1.3.1
[24]. Scheel H. and Fukuda T., Crystal Growth Technology, John Wiley & Sons, Sussex, UK, 2003.
[25]. Pang M., Bahr D., Lynn K., Effects of Zn addition and thermal annealing on yield phenomena of CdTe and Cd0. 96Zn0. 04Te single crystals by nanoindentation, Appl. Phys. Lett. 82, 1200 (2003)
[26]. Rai R., Mahajan S., Michel D., Smith H., McDevitt S., Johnson C.,Deformation behavior of CdTe and (Cd, Zn) Te single crystals between 200 and 600° C, Mater. Sci. Eng. B 10, 219 (1991)
[27]. Zhou S., Feng Y., Zhang L.,Growth and optical characterization of large scale crystal Cd x Zn 1− x S whiskers via vapor reaction, J. Cryst. Growth 252, 1 (2003)
[28]. Bera S.R. and Saha S., Influence of Growth Time in the Formation of CdTe Nanostructure, Nano Vision, Vol. 6(1), 1-9, 2016
[29]. Waterman, P.G. & Mole, S. (1994) Analysis of phenolic plant metabolites. Pp. 74–93 in Lawton JH & Likens GE (Eds.) Methods in Ecology. Blackwell Scientific Publication, Oxford.
[30]. Yao, L., Jiang, Y., Datta, N., Singanusong, R., Liu, X., Duan, J., Raymont, K., Lisle, A. & Xu, Y. (2004) HPLC analyses of flavonols and phenolic acids in the fresh young shoots of tea (Camellia sinensis) grown in Australia". Food Chemistry 84: 253–263.
[31]. Das T .K., Bhattacharya R., Manna A., Saha S., Role of reducing agent in the formation of ZnSe nanorods by chemical reduction method, Eur. Phys. J. Appl. Phys. 51, 30605 (2010) DOI: 10.1051/epjap/2010119
[32]. Pal R, Yadav S, Agnihotri A, Kumar D, Kumar A. , "Composition Dependence of Photoconductivity in Amorphous Se70Te30−xZnx Thin Films", Journal of Non-Oxide Glasses 1, 285 (2009).
[33]. Xu F. and Sun L., (2011), Solution-derived ZnO nanostructures for photoanodes of dye-sensitized solar cells, Energy Environ. Sci., 4, 818-841, DOI: 10.1039/C0EE00448K